Developmental Cell, Volume *28*

Supplemental Information

PI3K Class II α Controls Spatially Restricted Endosomal PtdIns3*P* and Rab11 Activation to Promote Primary Cilium Function

Irene Franco, Federico Gulluni, Carlo C. Campa, Carlotta Costa, Jean Piero Margaria, Elisa Ciraolo, Miriam Martini, Daniel Monteyne, Elisa De Luca, Giulia Germena, York Posor, Tania Maffucci, Stefano Marengo, Volker Haucke, Marco Falasca, David Perez-Morga, Alessandra Boletta, Giorgio R. Merlo, and Emilio Hirsch

Figure S1

A

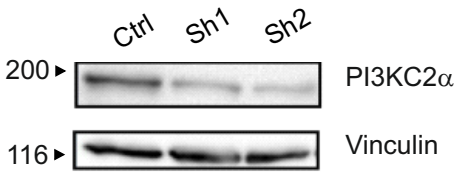
Ctrl
Sh1
Sh2
200
PI3KC2α
116
Vinculin

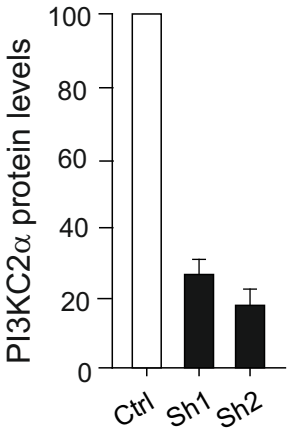
PI3KC2α protein levels
100
80
60
40
20
0
Ctrl
Sh1
Sh2

B

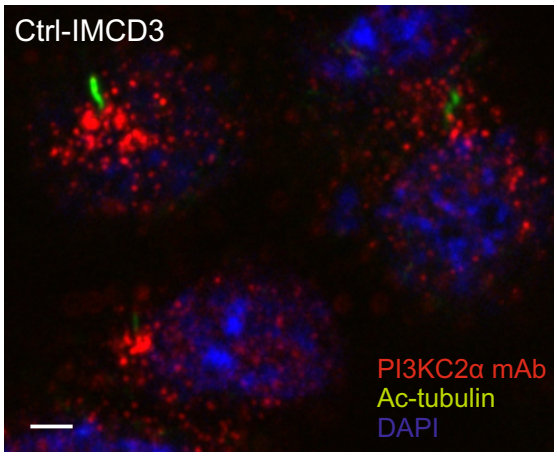
Ctrl-IMCD3
PI3KC2α mAb
Ac-tubulin
DAPI

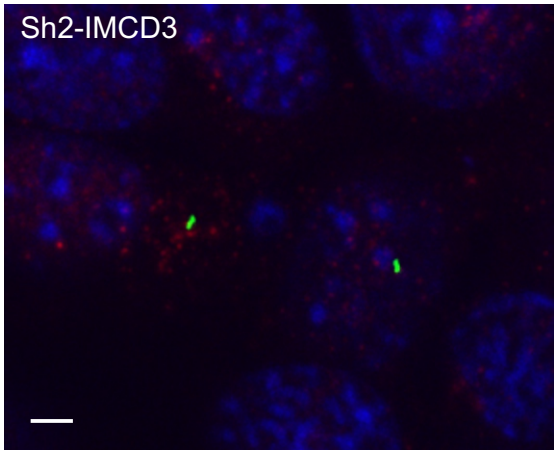
Sh2-IMCD3

Figure S1: Enrichment of PI3K-C2α around the ciliary base in IMCD3 cells. Related to Figure 1.**A**, Western blot analysis of PI3K-C2α protein expression in IMCD3 cells after lentiviral infection with either a control (Ctrl) sequence containing empty pGIPZ vector or two different shRNA sequences targeting the murine *Pik3c2a* transcript (Sh1 and Sh2). Quantification of PI3K-C2α down-modulation in 3 different infections is shown on the left. **B**, Staining of quiescent IMCD3 cells showing the primary cilium (acetylated α-tubulin, green) and endogenous PI3K-C2α (green). PI3K-C2α localizes around the ciliary base in Ctrl-IMCD3, while signal is severely reduced in Sh1 and Sh2 cells (red Bar=300 nm).

Figure S2

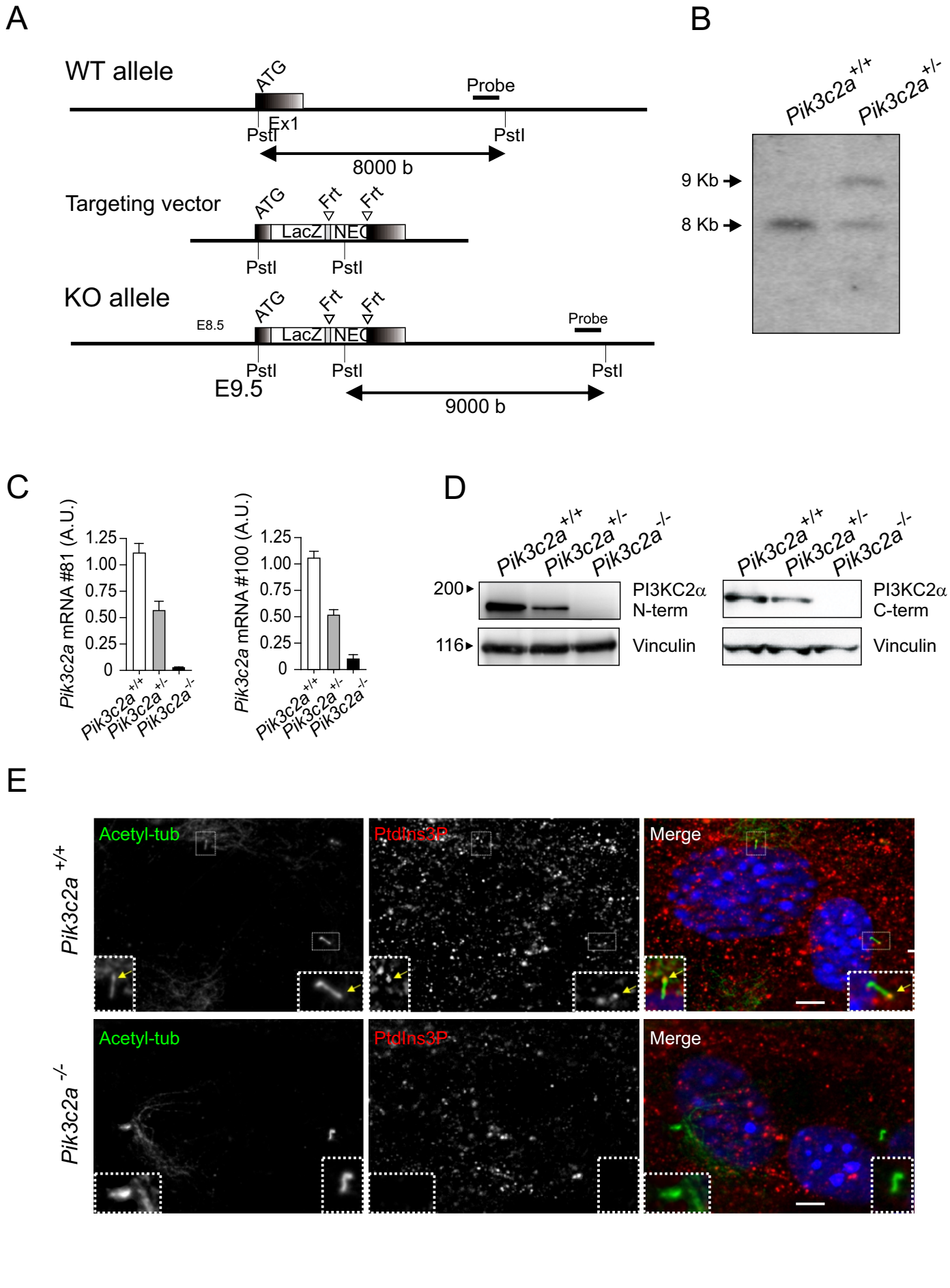
A
WT allele
ATG
Probe
Ex1
PstI
PstI
8000 b
Targeting vector
ATG
Frt
Frt
LacZ
NEO
PstI
PstI
KO allele
E8.5
ATG
Frt
Frt
LacZ
NEO
Probe
PstI
PstI
PstI
E9.5
9000 b
B
Pik3c2a+/+
Pik3c2a+/-
9 Kb
8 Kb
C
Pik3c2a mRNA #81 (A.U.)
1.25
1.00
0.75
0.50
0.25
0
Pik3c2a+/+
Pik3c2a+/-
Pik3c2a-/-
Pik3c2a mRNA #100 (A.U.)
1.25
1.00
0.75
0.50
0.25
0
Pik3c2a+/+
Pik3c2a+/-
Pik3c2a-/-
D
Pik3c2a+/+
Pik3c2a+/-
Pik3c2a-/-
200
PI3KC2α N-term
116
Vinculin
Pik3c2a+/+
Pik3c2a+/-
Pik3c2a-/-
PI3KC2α C-term
Vinculin
E
Pik3c2a+/+
Acetyl-tub
PtdIns3P
Merge
Pik3c2a-/-
Acetyl-tub
PtdIns3P
Merge

Figure S2: Details of the gene targeting strategy and expression of PI3K-C2α in *Pik3c2a*-mutants. Related to Figure 2. **A**, Schematic drawing of the murine *Pik3c2a* wild-type allele (top), of the targeting vector engineered for homologous recombination (mid) and of the modified allele after recombination. A *lacZ* (bacterial β-galactosidase) reporter-*neoR* cassette was inserted in-frame with the endogenous ATG start codon (exon 1 of *Pik3c2a*). A probe for screening of neomycin-resistant ES clones (shown as a black bar) was designed to detect an 8 kb and a 9 kb fragment in the wild-type and the recombinant allele, respectively, upon digestion of the genomic DNA with PstI. **B**, Southern blot analysis of genomic DNA from wild-type and heterozygous ES cells. **C**, Quantification of *Pik3c2a* mRNA in samples from wild-type, *Pik3c2a*$^{+/-}$ and *Pik3c2a*$^{-/-}$ embryos at the 1-5 somite stage by qPCR. To amplify *Pik3c2a* transcript, two specific assays were designed: assay #81 amplified a cDNA sequence comprising exon1/2 junction (left), while assay #100 comprised the exon 12/13 junction (right). A 50% reduction is observed in heterozygous embryos while in the null embryos the *Pik3c2a* mRNA is nearly undetectable . **D**, Western blot analyses of PI3K-C2α protein expression in wild-type, *Pik3c2a*$^{+/-}$ *Pik3c2a*$^{-/-}$ embryos is evidenced with two different antibodies recognizing either the N-terminal (left) or the C-terminal (right) portion of PI3K-C2α. Equal loading was monitored by vinculin expression. A reduction of the PI3K-C2α protein level is observed in heterozygous, while complete loss is evidenced in *Pik3c2a*$^{-/-}$ samples. **E,** Immunofluorescence labeling the PI3K-C2α product PtdIns3*P* (red) at the base of the primary cilium (acetylated α-tubulin, green). Bar=200 nm.

Figure S3

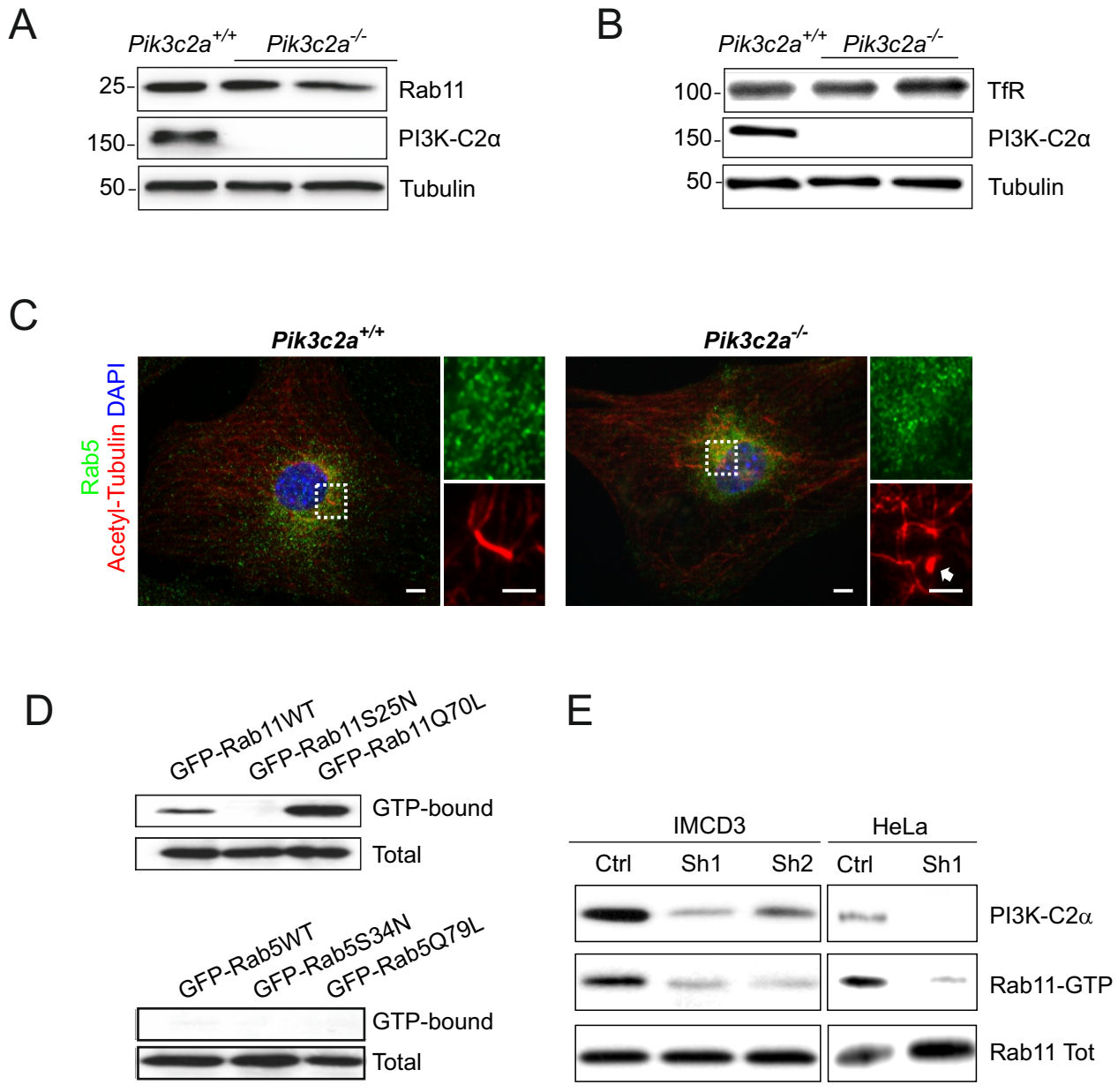
A
Pik3c2a+/+
Pik3c2a-/-
25-
Rab11
150-
PI3K-C2α
50-
Tubulin
B
Pik3c2a+/+
Pik3c2a-/-
100-
TfR
150-
PI3K-C2α
50-
Tubulin
C
Pik3c2a+/+
Pik3c2a-/-
Rab5
Acetyl-Tubulin DAPI
D
GFP-Rab11WT
GFP-Rab11S25N
GFP-Rab11Q70L
GTP-bound
Total
GFP-Rab5WT
GFP-Rab5S34N
GFP-Rab5Q79L
GTP-bound
Total
E
IMCD3
HeLa
Ctrl
Sh1
Sh2
Ctrl
Sh1
PI3K-C2α
Rab11-GTP
Rab11 Tot

Figure S3: Specific role of PI3K-C2α in Rab11 activation and localization. Related to Figure 3. **A,** Immunoblotting to detect Rab11 protein levels in wild-type and *Pik3c2a*$^{-/-}$ primary MEFs. Tubulin is shown for normalization. **B.** Immunoblotting to detect Transferrin Receptor (TfR) protein levels in membrane fraction enriched extracts from wild-type and *Pik3c2a*$^{-/-}$ primary MEFs. **C**, Immunofluorescence of serum deprived MEFs displayed comparable localization of Rab5 (green) in wild-type and *Pik3c2a*$^{-/-}$ MEFs. Higher magnification on the right show that Rab5 localization is not altered in the region around the base of the primary cilium (acetylated α-tubulin, red). Bar= 200 nm. **D,** Specificity of the pull down assay to detect GTP-bound Rab11 was tested in cell extracts from Hek293T cells transfected with GFP-Rab11 mutants (top): WT (GFP-Rab11WT), dominant negative (GFP-Rab11S25N), constitutively active (GFP-Rab11Q70L). The same experiment was performed using GFP-Rab5 mutants (WT, S34N, Q79L) as a negative control (bottom). **E,** Pull down experiment showing the endogenous content of Rab11-GTP either in IMCD3 cells (left) infected with either a control sequence (empty-pGIPZ) or shRNAs downmodulating PI3K-C2α (Sh1 and Sh2) or in Hela cells (right) infected either with control (empty-pGIPZ) or Sh1 sequence.

Figure S4

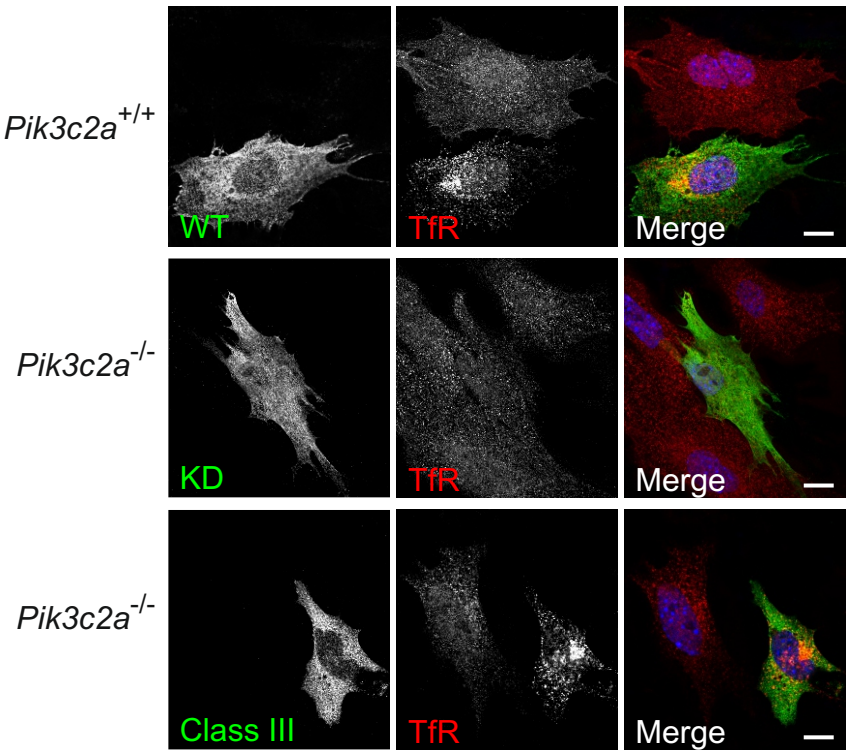
Pik3c2a+/+
WT
TfR
Merge
Pik3c2a-/-
KD
TfR
Merge
Pik3c2a-/-
Class III
TfR
Merge

Figure S4: PI3K-C2α-dependent PtdIns3P is necessary for Transferrin Receptor localization. Related to Figure 4. Localization of endogenous TfR (red) in *Pik3c2a*$^{-/-}$ MEFs transfected with either wild type, kinase inactive (KD) or Class III mutated (CIII) PI3K-C2α-GFP (green). Only PI3K-C2α forms able to produce PtdIns3P (WT and CIII) can rescue TfR accumulation at the pericentriolar compartment. Bar=200 nm.

Figure S5

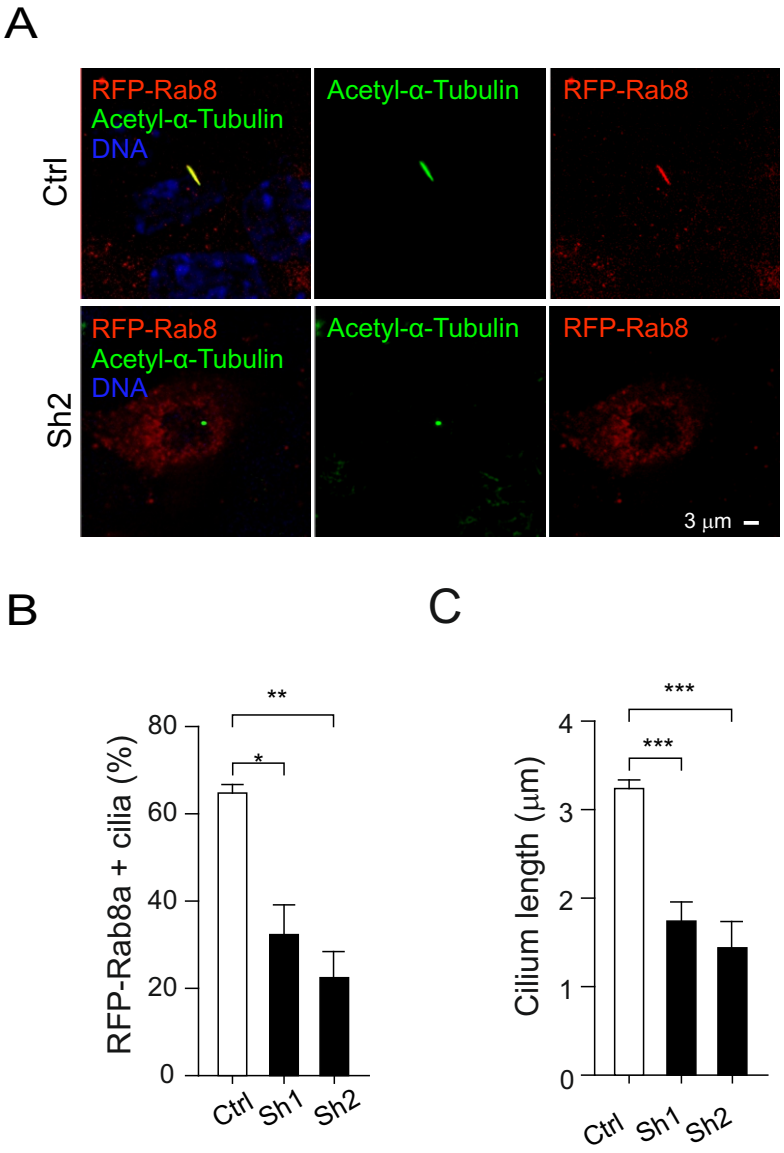
A
Ctrl
Sh2
RFP-Rab8
Acetyl-α-Tubulin
DNA
Acetyl-α-Tubulin
RFP-Rab8
3 μm
B
RFP-Rab8a + cilia (%)
80
60
40
20
0
**
*
Ctrl
Sh1
Sh2
C
Cilium length (μm)
4
3
2
1
0
***
***
Ctrl
Sh1
Sh2

Figure S5: Silencing of PI3K-C2α impairs ciliary localization of Rab8 and cilium elongation in IMCD3 cells. Related to Figure 5. **A**, Immunofluorescence of RFP-Rab8 (red) and acetylated α-tubulin (green) in 24h starved IMCD3. Bar=300 nm. **B**, Quantification of Rab8 positive cilia (n=30/group, 3 indepenent experiments). Concomitantly to cilia formation, Rab8 localizes at the cilium axoneme in 70% of Ctrl-infected IMCD3 cells, while only 35% and 30% of cilia were positive for Rab8 in *Pik3c2a* silenced Sh1 and Sh2-IMCD3 cells, respectively. **C**, Analysis of cilium length in Ctrl- and *Pik3c2a* silenced (Sh1 and Sh2) IMCD3 cells.

Figure S6

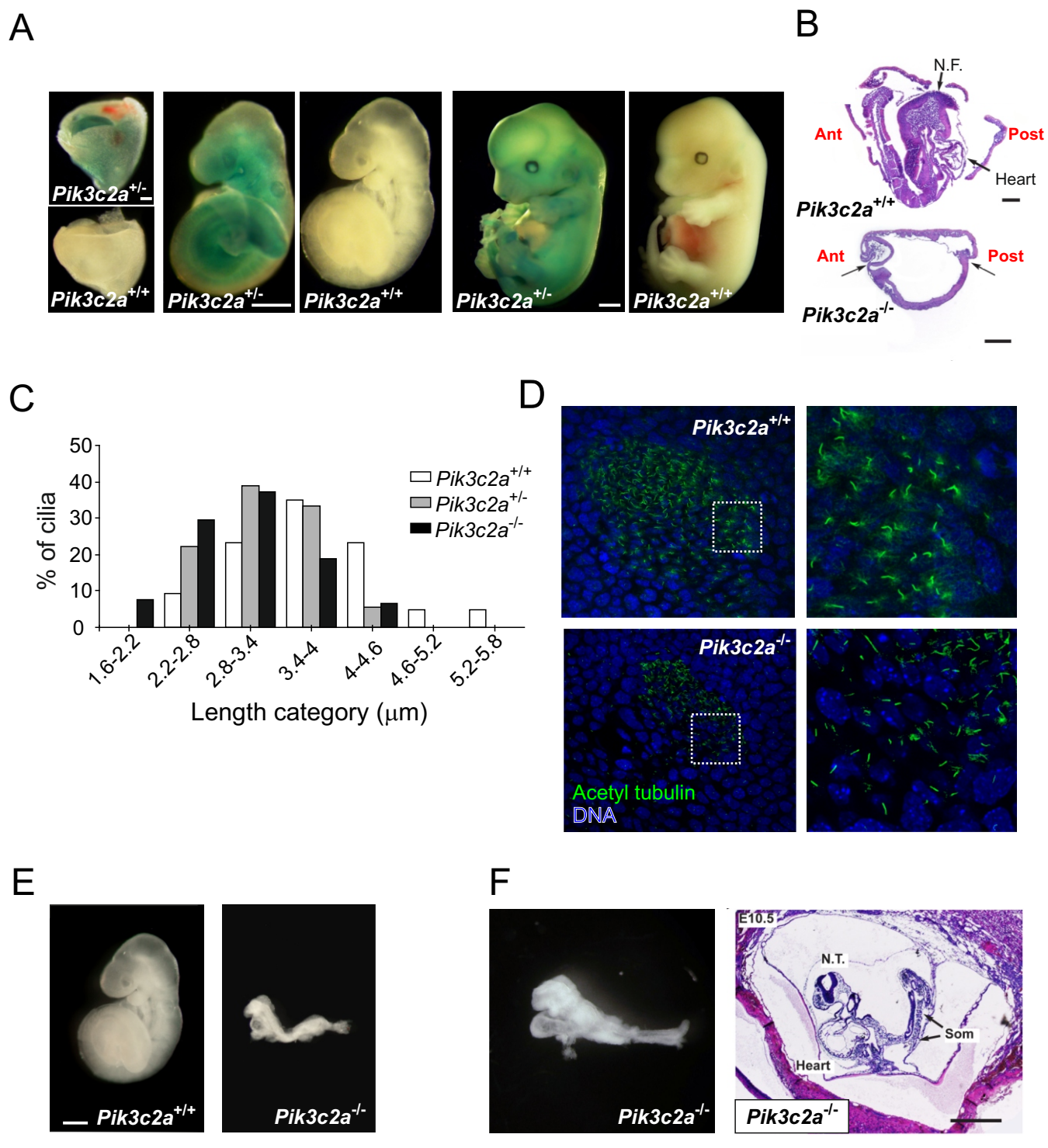
A
Pik3c2a+/-
Pik3c2a+/+
Pik3c2a+/-
Pik3c2a+/+
Pik3c2a+/-
Pik3c2a+/+
B
N.F.
Ant
Post
Heart
Pik3c2a+/+
Ant
Post
Pik3c2a-/-
C
% of cilia
50
40
30
20
10
0
Pik3c2a+/+
Pik3c2a+/-
Pik3c2a-/-
1.6-2.2
2.2-2.8
2.8-3.4
3.4-4
4-4.6
4.6-5.2
5.2-5.8
Length category (μm)
D
Pik3c2a+/+
Pik3c2a-/-
Acetyl tubulin
DNA
E
Pik3c2a+/+
Pik3c2a-/-
F
Pik3c2a-/-
E10.5
N.T.
Som
Heart
Pik3c2a-/-

Figure S6: Ciliary defects and developmental abnormalities of *Pik3c2a* mutant embryos. Related to Figure 6. **A,** Sections of wild-type and *Pik3c2a*-null embryos are compared at the same age (E8.5). Ant and Post indicate the anteriorposterior orientation. N.F., Neural Folds. **B**, Distribution of *Pik3c2a-lacZ* expression in *Pik3c2a*$^{+/-}$ embryos at E8.5, E9.5 and E13.5, detected by X-gal staining. Wild-type embryos at the same age are also shown for comparison. Scale bars correspond to 200 μm (E8.5), 500 μm (E9.5), 1 mm (E13.5) **C**, Graph showing the distribution of ciliary lengths expressed in percent over the total (n=30 cilia for each genotype). Measurement of ciliary length of ventral node cilia were obtained by scanning electron microscopy of wild-type, *Pik3c2a*$^{+/-}$ and *Pik3c2a*$^{-/-}$ presomite stage embryos (Main Figure 6A). Frequency peak of wild-type cilia is at 2.8-3.4 mm, while peaks of heterozygous and homozygous *Pik3c2a* cilia are shifted on the left (2.2-2.8 mm). Very short cilia (1.5-2 mm) are found only in *Pik3c2a*$^{-/-}$ embryos. Distribution of wild-type vs *Pik3c2a*$^{+/-}$ and wild-type vs *Pik3c2a*$^{-/-}$ cilia are significantly different according to Kolmogorov-Smirnov test (p= 5,70E-007 and p=0.009338 respectively). **D**, Whole mount staining of wild-type and *Pik3c2a*$^{-/-}$presomite stage embryos with Acetyl α-Tubulin (green) to visualize cilia of the ventral node. Higher magnification of the region delimited by the white square is shown on the left. **E,** E9.5 *Pik3c2a*$^{-/-}$ embryos are growth retarded as compared to wild-type littermates (left panel) and fail to undergo axial rotation and turning. Bar=500 μm. **F**, Unturned *Pik3c2a* embryos at E10.5. Micrograph on the left show a *Pik3c2a*$^{-/-}$ embryo with unlooped cardiac tube. Sagittal section on the right shows a distinct *Pik3c2a*$^{-/-}$ embryo displaying elevated somite number(>15) and closed neural tube in an unturned embryo. N.T., Neural Tube. Som, somites. Bar= 100 μm

Figure S7

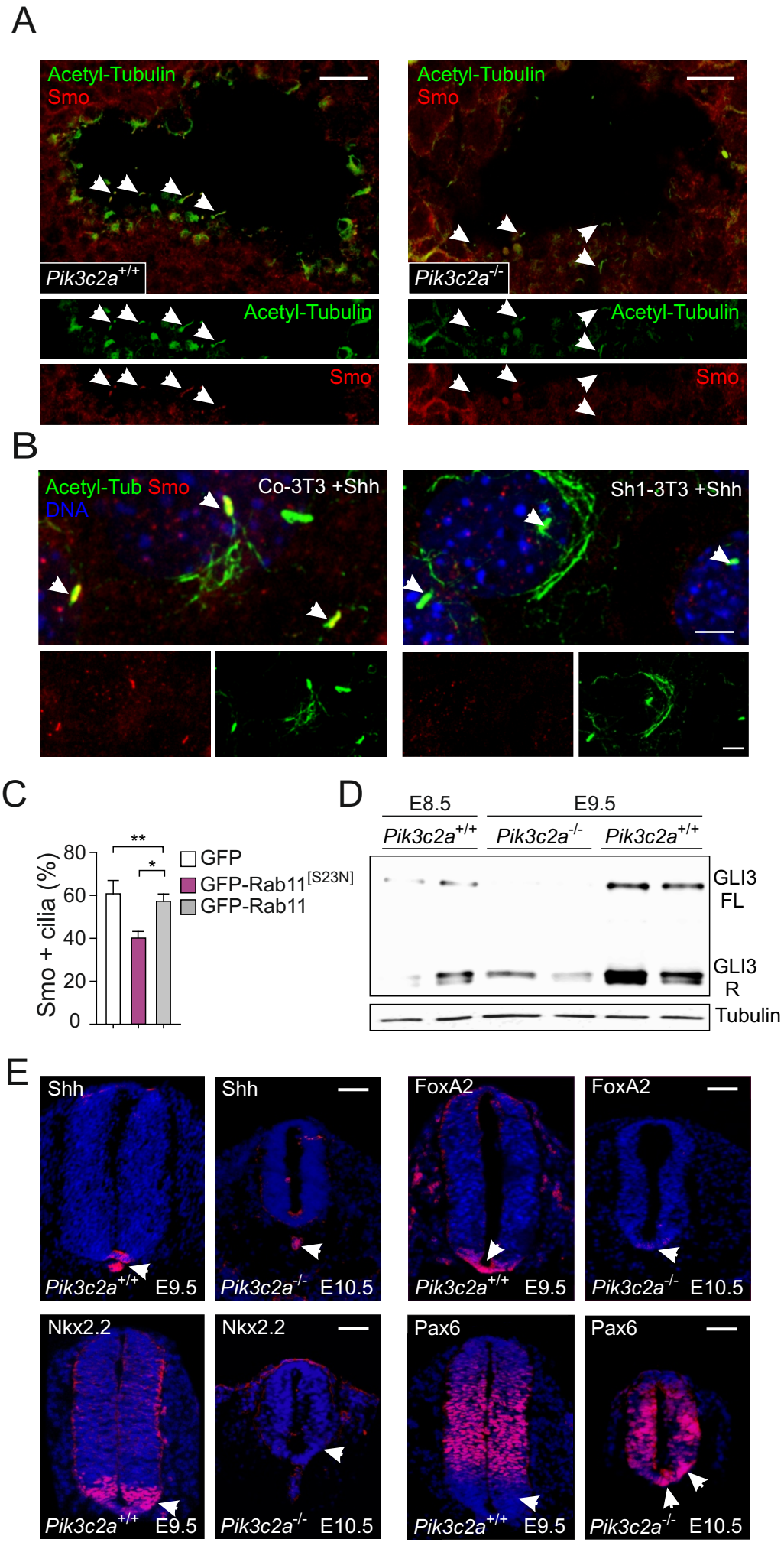
A
Acetyl-Tubulin
Smo
Pik3c2a+/+
Acetyl-Tubulin
Smo
Pik3c2a-/-
Acetyl-Tubulin
Smo
Acetyl-Tubulin
Smo
B
Acetyl-Tub Smo
DNA
Co-3T3 +Shh
Sh1-3T3 +Shh
C
Smo + cilia (%)
80
60
40
20
0
**
*
GFP
GFP-Rab11[S23N]
GFP-Rab11
D
E8.5
E9.5
Pik3c2a+/+
Pik3c2a-/-
Pik3c2a+/+
GLI3 FL
GLI3 R
Tubulin
E
Shh
Pik3c2a+/+ E9.5
Shh
Pik3c2a-/- E10.5
FoxA2
Pik3c2a+/+ E9.5
FoxA2
Pik3c2a-/- E10.5
Nkx2.2
Pik3c2a+/+ E9.5
Nkx2.2
Pik3c2a-/- E10.5
Pax6
Pik3c2a+/+ E9.5
Pax6
Pik3c2a-/- E10.5

Figure S7: Sonic Hedgehog signalling defects in *Pik3c2a*-deficient embryos. Related to Figure 7. **A**, Localization of Smoothened (Smo, red) and Acetyl-Tubulin (green) at the ventral node cilia in wild-type (micrographs on the left) and *Pik3c2a*$^{-/-}$ (on the right) embryos at the pre-somite stage by whole mount immunofluorescence. Smo accumulates along the cilium in wild-type cilia, while cilia of *Pik3c2a*$^{-/-}$ embryos are negative for Smo. The merge (top) and the single channel images (below) are shown. Scale bars=10 μm. **B**, Immunofluorescence using Smoothened (Smo, red) and Acetyl-Tubulin (green) antibodies to detect ciliary accumulation of Smo upon stimulation with the Hh pathway activator SAG (4 hours 100 nM) in control and *Pik3c2a*-silenced NIH 3T3 cells. **C**, Quantification of Smo positive cilia in NIH 3T3 cells transfected with either the dominant negative mutant of Rab11 (GFP-Rab11^{S25N}) or control plasmids (GFP-empty or GFP-Rab11^{WT}). After transfection, cells were starved for 48 hours to allow ciliation, then stimulated with SAG 100 nM for 4 hours. Provided is the mean % of three independent experiment. At least 90 cilia/genotype have been counted. **D**, Western blot analysis of Gli3 cleavage in *Pik3c2a*$^{-/-}$ embryos. Gli3 total levels in *Pik3c2a*$^{-/-}$ embryos at E9.5 were reduced as compared to wild-type littermates (5th and 6th lane). However total Gli3 levels were comparable to levels found E8.5 wild-type embryos, consistent with embryonic morphology (see Figure S6). *Pik3c2a*$^{-/-}$ embryos show increased Gli3 R/ Gli3 FL ratio, in agreement with reduced Hh pathway activation. **E**, Neural tube patterning of *Pik3c2a*$^{-/-}$ embryos. Transversal sections of E10.5 *Pik3c2a*$^{-/-}$ embryos at the level of the heart showed reduced size and developmental retardation. Wild-type sections suitable for comparison were cut from E9.5 embryos at the level of the heart. Staining with antibodies to Shh (upper left panels) showed that the protein was correctly produced in the notochord (arrows), while it was absent in the floorplate of *Pik3c2a*$^{-/-}$ embryos. Markers of ventral neurons FoxA2 (upper right) and Nkx2.2 (lower left) were undetectable, while the dorsal marker Pax6 (lower right) was present in the ventral neural tube of *Pik3c2a*$^{-/-}$ embryos. Bar= 50 μm

SUPPLEMENTAL TABLES

Table S1: Phenotype of *Pik3c2a*-mutant embryos. Related to Figure 6.

Genotyping of living progeny from *Pik3c2a*$^{+/-}$ crosses

Age	*Pik3c2a*$^{+/+}$	*Pik3c2a*$^{+/-}$	*Pik3c2a*$^{-/-}$	n
E9.5	26 (28%)	45 (48%)	23 (24%)	94
E10.5	43 (27%)	81 (51%)	35 (22%)	159
E11.5	100 (28%)	194 (54%)	66 (18%)	360
E12.5	15 (41%)	22 (59%)	0 (0%)	37
E13.5	17 (39%)	26 (61%)	0 (0%)	43
4 Weeks	212 (39%)	335 (61%)	0	547

Summary of laterality defects in *Pik3c2a*$^{-/-}$ embryos

	Complete	Incomplete	Absent	n	Age
Turning	0		23 (100%)	23	E9.5
	2 (4%)	7 (17%)	32 (78%)	41	E10.5
	7 (15%)	7 (15%)	31 (70%)	45	E11.5
Cardiac Looping	15 (39%)		25 (61%)	41	E10.5
Nodal expression	0		6	6	1-5 somites
Lefty 1/2 expression	0		4	4	1-5 somites
Shh expression	4		0	4	1-5 somites

EXTENDED EXPERIMENTAL PROCEDURES

Generation of Pik3c2a knock-out mice.

A lacZ (bacterial β-galactosidase)-neoR cassette was inserted in-frame with the ATG start codon of *Pik3c2a* via bacterial recombination. The targeting vector was electroporated in 129-strain mouse ES cells, clones were selected for neomycin resistance and screened by Southern blot (Suppl. Fig. 1b). Chimeric founders were obtained by standard blastocyst injection and readily transmitted the mutation in the germ line. Wild type and targeted alleles were genotyped by tail PCR with specific primers. Given are the primer sequences and the approximate lengths of the amplified DNA fragments. Fw: AAGATGTGAACAAAGCAGAAGCGTTAC; rev wild type specific (590 bp): GTTTACCAGTCTATCGGCCACTAGTCAGT; rev knock-out specific (972 bp): TATGCAGCAACGAGACGTC. Mice were backcrossed for 8 generations in the C57BL6J genetic background. Neo cassette flanked by Frt sites was removed by crossing with transgenic mice expressing the Flp recombinase under beta-actin promoter (B6.Cg-Tg(ACTFLPe)9205Dym/J). Neo removal was verified by specific PCR using the following primers: fw:GGGAGGATTGGGAAGACAAT; rev: TGTTCTGAGCCCTTCGTTCT, that produced a 265 bp amplicon only in Neo positive mice. *Pik3c2a*-ΔNeo mice were backcrossed with C57BL6 mice for one generation to lose the Flp transgene. Primers for Flp genotyping: fw: GAGACAAAGACAAGCGTTAGTAGG; rev: GTGCGAAGTAGTGATCAGGTATTG. Studies were performed in littermates from heterozygous crosses.

Expression vectors

The *mGFP-2xFYVE* construct was obtained from Dr. T. Balla (NIH, Bethesda MD, USA), the *GFP-Rab11, GFP-Rab11[Q70L]* and *GFP-Rab11[S25N]* were obtained from Dr. R. Bonecchi (Humanitas, Rozzano, Italy), *GFP-Rab5[Q79L]* was obtained from Dr Letizia Lanzetti (IRCC, Candiolo, Italy), GST-Rab11 plasmid was a kind gift of Dr G. Scita (IFOM, Milan, Italy). Plasmids

for ISH probes were obtained from Dr S. Piccolo (Università di Padova, Italy). Wild-type PI3K-C2α-GFP plasmid was obtained from Dr M. Falasca and engineered as in (Gaidarov et al., 2005) to obtain PI3K-C2α^{KD}. PI3K-C2α^{cIII} was engineered as described in (Posor et al., 2013). Briefly, PI(3)K C2a was mutated from 1283KRDR1286 to 1283KPLP1286 in order to introduce putative PI head-group interaction sites from class III PI3Ks within the core catalytic center of PI3K-C2α.

Immunofluorescence

Immunofluorescence of PFA 4% fixed primary MEFs and IMCD3 cells followed standard procedures. Primary antibodies: anti-Acetylated-Tubulin monoclonal (6-11B-1, Sigma, St. Louis MO, USA), anti-Acetylated-Tubulin polyclonal D20G3 (Cell Signaling), anti-γ-Tubulin monoclonal (GTU-88, Sigma), anti-PI3K-C2α monoclonal (anti p170 #611046 BD Transduction Laboratories), anti-Rab11a polyclonal (Abcam, Inc Cambridge MA), anti-Rab11a monoclonal (BD Transduction Laboratories #610657), anti-Rab5 monoclonal (D11, Santa Cruz Biotechnology), anti-PtdIns3*P* monoclonal (Echelon), anti-Transferrin Receptor polyclonal (Sigma). Anti-GFP and anti-Vinculin are homemade produced. Secondary antibodies were: goat anti-rabbit and goat anti-mouse, labelled with Alexa-350, -488 or -568 (Molecular Probes/Invitrogen). Cells were stained with DAPI and examined with either Zeiss Observer-Z1 microscope, equipped with the Apotome or Leica TCS-II SP5 confocal microscope. Raw images were digitally processed only to normalize the background and enhance the contrast. Z-stacks were acquired and processed with the Maximum Projection tool. 3D morphometric measurement of ciliary length was performed with Filament tool of Imaris (BitPlane, Zurich, Switzerland). To assess PtdIns3P abundance around the ciliary base, fluorescence intensity of GFP-2XFYVE was calculated with Imaris, Surface tool, as follows. 3D pictures taken with fixed exposure time where processed to measure the green fluorescent intensity around the ciliary base in a region with standard dimensions (diameter 8μm, depth 10 μm). At least 25 photo/genotype were taken in three independent experiments and the results were reported in figure 2B.

In situ localization of Smo and acetylated-Tubulin in nodal cilia was done on embryos at the presomite stage essentially as described (Corbit et al., 2005). For 3D imaging, embryos were mounted in 0.5% low-melting agarose. Anti-Smo primary antibody was A2666 and A2668 (Lifespan Biosciences, Seattle WA, USA). Analysis of Smo localization in NIH 3T3 cells was performed as follows: lentivirus-infected or wild-type NIH 3T3 were plated at subconfluence and transfected with Effectene as described in the section “Shh stimulation”. After 8-12 hours, cells were serum starved (DMEM 1% FBS) for 48 hours to allow ciliation, then stimulated for 4 hours with 100 nM SAG (Calbiochem) diluted in starve medium to promote Smo translocation to cilia. Immunofluorescence was performed essentially as described in (Milenkovic et al., 2009). Affinity purified rabbit polyclonal antisera against mouse Smo (anti-SmoC) was a kind gift of R. Rohatgi. As negative controls, unstimulated cells were stained. Quantification of Smo positive cilia in transfected cells was performed in blind, as follows: GFP positive cells were scored for the presence of Smo on cilia. The percentage of Smo positive cilia was estimated as: number of positive cilia/10 counted cilia *100. At least 90 cells/condition were counted in 3 independent experiments and the mean and standard error were provided. For neural-tube analyses, E9.5 and E10.5 embryos were fixed for 2 hours in PFA 4%, rinsed in PBS, equilibrated overnight at 4°C in PBS with 30% sucrose, embedded in OCT Tissue Freezing Medium (Tissue Tek) and cutted (20 μm). For FoxA2, Nkx2.2 and Pax6 staining, cryosections were subjected to antigen retrieval (1 h 80°C in 10mM NaCitrate buffer), permeabilization (30 mins, room temperature, in PBS 0.3% Triton X100), blocking (30 mins, room temperature, 2% Triton, 2% BSA, 1% goat serum) and incubated in primary antibody diluted in blocking buffer overnight at 4°C. For Shh staining antigen retrieval was avoided. Primary antibodies to Shh (pure), FoxA2 (1:20), Nkx2.2 (1:20) were non concentrated hybridomas from Developmental Studies Hybridoma Bank, University of Iowa. Polyclonal primary ab to Pax6 (1:1000) was from Chemicon. Embryo sections were imaged with a Leica TCS-II SP5 confocal microscope.

Western blotting

Protein extraction, SDS-PAGE and western blotting followed standard procedures. Antibodies: anti-PI3K-C2α monoclonal (anti p170 #611046 BD Transduction Laboratories), anti-PI3K-C2α polyclonal (PI3 kinase C2 alpha antibody [C3], C-term, GTX104640, GeneTex, Irvine, CA, USA) polyclonal anti-Gli3 (AF3690, R&D systems, Inc), anti-Rab11a monoclonal (BD Bioscience #610657), polyclonal anti-Transferrin Receptor (Sigma).

In situ hybridization

For ISH, pregnant females were sacrificed considering the morning of the vaginal plug as E0.5. Embryos were dissected and staged based on morphology and on somite counting. Experiments were performed on wild-type and mutant embryos that showed same number of somites (1-5). Hybridization followed the protocol provided in (www.hhmi.ucla.edu/derobertis/), with few modifications to allow genotyping after staining. Probes were prepared as digoxygenin (DIG)-UTP (Roche, Indianapolis IN, USA)-labeled antisense RNA probes, by in vitro transcription (Promega, Madison, WI, USA). Signal was revealed using AP-conjugated anti-DIG (Boehringer Mannheim, Germany) and developed with NBT-BCIP (Roche). At least four embryos per genotype were examined with each probe. Plasmid to produce mouse *Lefty1/2, Nodal* and *Shh* RNA were obtained by S. Piccolo (Morsut et al., 2010).

Gli3R/Gli3FL measurement

Experiments were performed on wild-type and mutant embryos that showed same number of somites (1-5), *Pik3c2a*$^{-/-}$ embryos were from E9.0-E9.5 litters from *Pik3c2a*$^{+/-}$ X *Pik3c2a*$^{+/-}$ crosses, wild-type embryos were at E8.5 from *Pik3c2a*$^{+/+}$ X Pik3c2a$^{+/+}$ crosses. Extra-embryonic tissue was removed and used for genotyping. Embryos were frozen in liquid nitrogen. After genotyping, 3 *Pik3c2a*$^{+/+}$ and 3 *Pik3c2a*$^{-/-}$ were pulled together and protein extraction was performed by resuspending samples in 20 μl laemely 2X buffer and 10’ incubation at 95°C. DNA fragmentation

was achieved by vortexing 1', high speed, for 3 times, during the 95°C incubation. Whole lysate was loaded in 6% acrylamide gel. Immunoblot was performed with polyclonal anti-Gli3 (AF3690, R&D systems, Inc) and secondary anti-Goat. Quantification of band intensity was performed with Quantity One 1-D Analysis software (Biorad), after checking that the intensity was within the linear range. Value obtained for the 87 kDa band (Gli3R) was divided for the value obtained for the 190 kDa band (Gli3FL). In Figure S7B, 1-5 somite *Pik3c2a*$^{+/+}$ and *Pik3c2a*$^{-/-}$ embryos were collected as described. *Pik3c2a*$^{+/+}$ E9.5 embryos were littermates of *Pik3c2a*$^{-/-}$1-5 somite embryos. All embryos were processed together for protein extraction, but *Pik3c2a*$^{+/+}$ E9.5 embryos were lysed in 100 µl laemely 2X buffer and only 20 µl of total extract were loaded in order to load similar amounts of total protein. Comparable loading was assessed by immunoblotting of Tubulin (anti-α-Tubulin, monoclonal, homemade).

Gene expression in single embryos

Wild-type, *Pik3c2a*$^{+/-}$, *Pik3c2a*$^{-/-}$ embryos were dissected clean of extra-embryonic tissues (used for genotyping), staged and collected individually in RNA-later (Invitrogen, Carlsbad CA, USA). Embryos displaying 1-5 somites were used to extract total RNA using the TriPure Reagent (Roche) followed by isopropanol precipitation. RNA was quantified and subjected to Real-Time qPCR as indicated below. Relative abundance of *Ptch1, Gli1, Fgf8* and *Pik3c2a* mRNAs was determined as described below. mRNA input was normalized with *TATA-binding protein* mRNA.

Real-time qPCR.

For Real-time qPCR analyses, retrotranscription was done with High-Capacity cDNA RT kit (Applied Biosystems, Foster City, CA, USA). Relative mRNA abundance was determined by Real-Time qPCR, using the ABI Prism 7900 Real-Time PCR system (Applied Biosystems) with Taqman assays from the Universal Probe Library (Roche). Primer sequences are listed above.

Gene name	**Gene code**	**Left primer**	**Right Primer**
Pik3c2a #81	NM_011083.2	cattcggacagctcaatttaca	tcccatttgggtctttctga

Pik3c2a #100	NM_011083.2	ggagctccttgatgcaaaat	tcatcactaatggcctccatc
TATA box binding protein	NM_013684.3	ggcggtttggctaggttt	gggttatcttcacacaccatga
Ptch1	NM_008957.2	ggaaggggcaaagctacagt	tccaccgtaaaggaggctta
Gli1	NM_010296.2	ctgactgtgcccgagagtg	cgctgctgcaagaggact
Fgf 8	NM_010205.1	tcctgcctaaagtcacacagc	tgagctgatccgtcacca
Smo	NM_176996.4	gcaagctcgtgctctggt	gggcatgtagacagcacaca

Shh stimulation

For Shh stimulation, MEFs from individual *Pik3c2a*$^{+/+}$, *Pik3c2a*$^{+/-}$ or *Pik3c2a*$^{-/-}$embryos were kept in culture for 7 days. One MEF clone for each genotype was plated in 2 separate wells (1x10^5 cells/well) and deprived of serum for 48 hrs. Medium was then replaced with either starve medium (control) or the same with 100 nM rm-Shh-N (R&D, Minneapolis MN, USA) (stimulated). Total RNA was extracted 24 hrs later with RNA mini-kit (Invitrogen). Real-Time qPCR analysis of *Ptch1, Gli1* and *Smo* mRNA abundance was performed as described in the section "*Real time qPCR"* of the Extended Experimental Procedures. *18s* rRNA was measured for each sample and used for internal normalization of RNA content. The sample from untreated *Pik3c2a*$^{+/+}$ MEFs was used as calibrator to calculate relative mRNA abundance of treated and untreated samples for the 3 genotypes. Then the fold induction for each MEF clone was calculated as follows: value obtained for each clone in Shh stimulated conditions was divided for the value obtained from the same clone in non stimulated conditions. This provides a single value representative of the increase in *Ptch1, Gli1* and *Smo* mRNA abundance after Shh stimulation for each clone (fold induction). In each experiment one clone of *Pik3c2a*$^{+/+}$, *Pik3c2a*$^{+/-}$ and *Pik3c2a*$^{-/-}$ MEFs was tested and the experiment was repeated 4 times. Graph bars represent the mean fold induction for each genotype.

For the rescue experiment of Shh response, NIH 3T3 cells were infected with either control (pGIPZ empty) or sh1 sequence to silence *Pik3c2a,* as described. Cells at 3rd passage after infection were plated 100.000/well on 12-well-plates, transfected with Effectene Transfection Reagent with 0.8-1.5 µg of plasmid DNA to express Rab11 WT, Rab11 Q70L, PI3K C2α CIII. 12h after transfection, cells were serum-starved (DMEM 1% bovine serum) for 36 h, then stimulated with 100 nM rm-

Shh-N for 24 hours and harvested for RNA extraction and *Ptch1, Gli1* and *Smo* mRNA analysis as described above.

Lentiviral infection

Plasmids containing shRNA sequences against Mm *Pik3c2a* were purchased from Thermo Scientific. For packaging, sequences in pGIPZ vector were transfected in 293T cells together with the packaging (pCMV-dR8.74) and envelope (VSV-G) vectors. After 48h, 293T medium was filtered through a 0.4 μm pore filter and concentrated by 3h centrifugation at 50.000g. NIH 3T3, IMCD3 and HeLa cells were incubated with virus for 48 h then selected with puromycin 2mg/ml for 7 days. Cells at early passages after infection (2^{nd}-3^{rd}) were used for experiments.

Scanning Electron Microscopy

Samples were fixed ON at 4°C in 2.5% glutaraldehyde, 0.1M cacodylate buffer (pH 7.2), and post-fixed in 2% OsO_4 in the same buffer. After serial dehydration in increasing ethanol concentrations, samples were dried at critical point, coated with platinum by standard procedures, and examined in a ESEM Tecnai Quanta 200 FEG (FEI).

Cell fractionation.

NIH 3T3 cells were gently homogenized in homogenization buffer (250 mM sucrose, 3 mM imidazole, 1mM EDTA pH 7.4) and post-nuclear supernatants (PNSs) were prepared. The PNSs were adjusted to 40.6% sucrose using a stock solution (62% sucrose, 3 mM imidazole, pH 7.4, 1 mM EDTA), loaded at the bottom of centrifugation tubes, then sequentially overlaid with 4 ml 35% solution (35% sucrose, 3 mM imidazole, pH 7.4, 0.5 mM EDTA), followed by 2.5 ml 25% solution (25% sucrose, 3 mM imidazole, pH 7.4, 0.5 mM EDTA), and finally filled up with homogenization buffer. The gradients were centrifuged at 108,000 g for 1 hours at 4°C. After centrifugation fractions were collected. The early endosome-enriched (EE) and the late endosome-enriched (LE) fractions were collected at the 35/25% and 25%/homogenization

interphase, respectively. Fractions were subjected to chloroform methanol precipitation. The ratio chloroform/methanol/water was 1:4:3. Protein was quantified and same amount of protein was loaded in SDS-PAGE followed by western blot analyses.

SUPPLEMENTAL REFERENCES

Corbit, K.C., Aanstad, P., Singla, V., Norman, A.R., Stainier, D.Y., and Reiter, J.F. (2005). Vertebrate Smoothened functions at the primary cilium. Nature *437*, 1018-1021.

Gaidarov, I., Zhao, Y., and Keen, J.H. (2005). Individual phosphoinositide 3-kinase C2alpha domain activities independently regulate clathrin function. J Biol Chem *280*, 40766-40772.

Milenkovic, L., Scott, M.P., and Rohatgi, R. (2009). Lateral transport of Smoothened from the plasma membrane to the membrane of the cilium. J Cell Biol *187*, 365-374.

Morsut, L., Yan, K.P., Enzo, E., Aragona, M., Soligo, S.M., Wendling, O., Mark, M., Khetchoumian, K., Bressan, G., Chambon, P., *et al.* (2010). Negative control of Smad activity by ectodermin/Tif1gamma patterns the mammalian embryo. Development *137*, 2571-2578.

Posor, Y., Eichhorn-Gruenig, M., Puchkov, D., Schoneberg, J., Ullrich, A., Lampe, A., Muller, R., Zarbakhsh, S., Gulluni, F., Hirsch, E., *et al.* (2013). Spatiotemporal control of endocytosis by phosphatidylinositol-3,4-bisphosphate. Nature *499*, 233-237.